

Ultra-high temperature compressive creep behavior of an in-situ Al_2O_3 single-crystal/YAG eutectic composite

Yoshihisa Harada^{a,*}, Takayuki Suzuki^a, Kazumi Hirano^a, Yoshiharu Waku^b

^a*Institute of Mechanical Systems Engineering, National Institute of Advanced Industrial Science and Technology (AIST), Tsukuba, Ibaraki 305-8564, Japan*

^b*Ube Research Laboratory, Corporate Research & Development, UBE Industries, Ltd, Ube, Yamaguchi 755-8633, Japan*

Received 17 April 2003; received in revised form 16 June 2003; accepted 6 July 2003

Abstract

Compressive creep tests were conducted for an in-situ single-crystal alumina/yttrium aluminum garnet [$\text{Al}_2\text{O}_3/\text{Y}_3\text{Al}_5\text{O}_{12}$ (YAG)] eutectic composite for a specimen with a compressive axis with 0 or 90° to the solidified direction at temperatures between 1723 and 1923 K under stress ranges of 140–450 MPa in air environments. The single-crystal Al_2O_3 /YAG eutectic exhibited a stress exponent of 5.4–10, indicative of compressive creep behavior characterized by a dislocation mechanism. Activation energies for creep deformation were 810–1024 kJ/mol, close to that for 42° from *c*-axis single-crystal Al_2O_3 or single-crystal YAG, in agreement with that of self-diffusion for *c*-axis single-crystal Al_2O_3 . The 0° specimen exhibited a slight decrease in creep rate by about half for a 90° specimen corresponding to results from crystal anisotropy in single-crystal Al_2O_3 . The Larson–Miller method provided an effective means of comparing creep resistance of oxides on the basis of results obtained under different stresses and temperatures.

© 2003 Elsevier Ltd. All rights reserved.

Keywords: Al_2O_3 ; Composites; Creep; Directional solidification; YAG

1. Introduction

In-situ single-crystal oxide ceramic eutectic composites such as Al_2O_3 /YAG, Al_2O_3 /GdAlO₃(GAP), Al_2O_3 /Er₃Al₅O₁₂(EAG), and Al_2O_3 /EAG/ZrO₂ have recently developed by Waku et al.^{1–6} For instance, the binary Al_2O_3 /YAG system is produced using an eutectic reaction composed of 82 mol% Al_2O_3 –18 mol% Y_2O_3 with a dimension of 40 mm in diameter and 80 mm in height having a new microstructure in which single-crystal Al_2O_3 and single-crystal YAG phase consist of fine lamellar and three-dimensional network structures. This composite is thermally stable even at 1973 K for 1000 h in air environments; it has an excellent flexural strength up to 400 MPa at 2000 K^{1–3} and good productivity in fabricating complex shape components compared with conventional sintered engineering ceramics. Such high performance composites are the most promising candidate for use as ultra-high temperature structural applications above 1773 K in oxidizing environments to

improve heat efficiency of aerospace jet engines or power generation gas turbines. However, a literature search reveals few studies investigating only creep behavior of in-situ single-crystal oxide ceramic eutectic composites in oxidizing environments.⁷

In this paper compressive creep tests were conducted for single-crystal Al_2O_3 /YAG eutectic composite at 1723–1923 K in air environments to elucidate ultra-high temperature creep deformation characteristics. Also, a direct comparison of creep results from different oxides was evaluated with the Larson–Miller normalization procedure.

2. Experimental procedures

High-purity commercial powders of α - Al_2O_3 (AKP-30; Sumitomo Chemical Co. Ltd., 99.99%) and Y_2O_3 (Y_2O_3 -SU; Shin-etsu Chemical Co., Ltd., 99.999%) were used for starting materials. These powders were ball-milled in ethanol with 82 mol% Al_2O_3 –18 mol% Y_2O_3 to form a composite with 50 vol.% of each phases. After removing ethanol and drying the slurry with a rotary evaporator, these powders were pre-melted to

* Corresponding author. Tel.: +81-298-61-7169; fax: +81-298-61-7853.

E-mail address: harada.y@aist.go.jp (Y. Harada).

yield an ingot which was then placed in a molybdenum crucible. It was fabricated by unidirectional solidification in a crucible using a Bridgman-type apparatus (Japan Ultra-high Temperature Materials Research Center, Ube, Japan) at a melting temperature of 2173 K, lowering the crucible at 1.39×10^{-6} m/s.^{1–3}

Cylindrical compressive creep specimens were machined into two types with their axis parallel to (0° specimen) and perpendicular to (90° specimen) the solidified direction. Nominal specimen sizes were approximately 4 mm in diameter and 8 mm in height. Surfaces of all specimens were polished to roughness of less than 10 μm . After machining and polishing, all specimens were heat-treated at 1873 K in air for 1 h. Constant-load compressive creep tests were conducted in air environments at temperatures of 1723–1923 K within the stress range from 140 to 450 MPa using a conventional PC-controlled MTS Materials Testing System (MTS810; MTS Japan, Ltd.) with a compact electric furnace (SS-1700-45; Nems Co., Ltd.). Compression rams were made from hardened alloy steel with sapphire rods. For platens, a combination of single-crystal YAG of [111] orientation and single-crystal $\text{Al}_2\text{O}_3/\text{YAG}$ eutectic of the 0° specimen to the solidified direction, with the single-crystal $\text{Al}_2\text{O}_3/\text{YAG}$ eutectic sandwiched between the sapphire rod and the YAG platen, was found to function best up to 1973 K. Test temperature was measured with two sets of B-type (Pt-Rh) thermocouples located in the near vicinity of the specimen. Temperature deviation was ± 1 K of the set point throughout each test after 1 h soak at the test temperature. Specimen strains were calculated from extensometric displacements measured using a linear variable differential transducer with resolution of 0.5 μm ; it was attached to the load train.

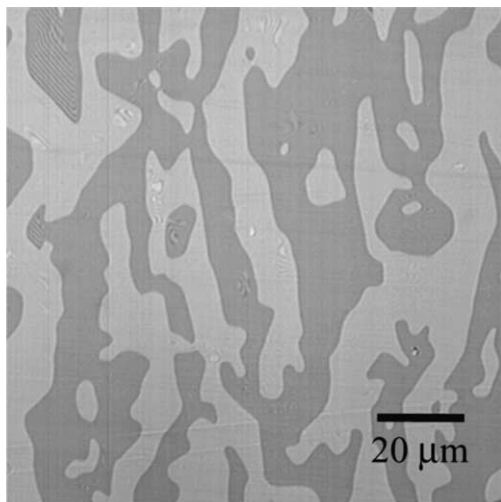


Fig. 1. SEM image of microstructure for single-crystal $\text{Al}_2\text{O}_3/\text{YAG}$ eutectic with the compressive axis parallel to the solidified direction. The dark phase is Al_2O_3 and the bright phase is YAG.

Microstructural observation was performed by scanning electron microscopy (Jeol6400Fs; Jeol, Ltd.) and transmission electron microscopy (Jeol200CX; Jeol, Ltd.). TEM foils were prepared by dimple polishing on one side and ion beam thinning of both sides. Density of creep specimens was measured by Archimedes' method in ethanol (99.8%) before and after creep testing. Specimens were cleaned in ethanol and dried prior to measurement. Density measurements of specimens indicated density of 4.30 ± 0.01 g/cm³ for single-crystal $\text{Al}_2\text{O}_3/\text{YAG}$ eutectic and no significant density changes after creep testing.

3. Results and discussion

3.1. Microstructure

Fig. 1 shows an SEM image of microstructure for single-crystal $\text{Al}_2\text{O}_3/\text{YAG}$ eutectic with the compressive axis parallel to the solidified direction. The white phase is YAG; the dark phase is Al_2O_3 . The figure shows that the microstructure has a fine lamellar structure consisting of 1–20 μm in width of each phase and no pores or colonies. A three-dimensional network structure is observed containing a single-crystal YAG distributed in a matrix of single-crystal Al_2O_3 determined by X-ray diffraction. Growth directions of Al_2O_3 and YAG are determined to be $[11\bar{2}0]$ and $[210]$, respectively.^{1–3} The parallel section seems to be elongated in the solidified direction.

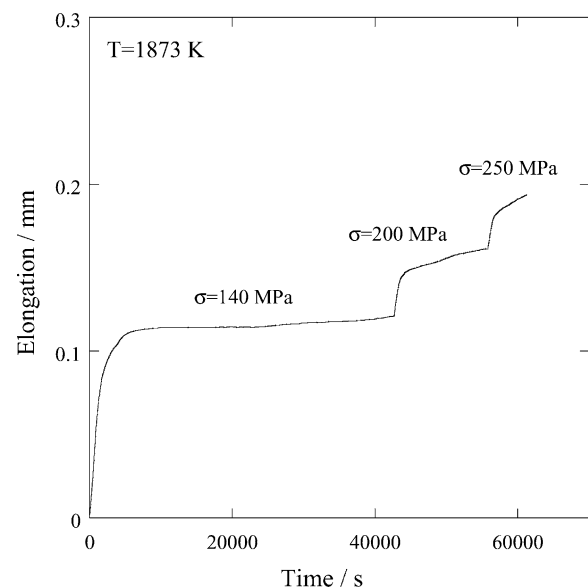


Fig. 2. Typical time vs. elongation curve for single-crystal $\text{Al}_2\text{O}_3/\text{YAG}$ eutectic of 0° specimen to the solidified direction for a compressive creep test at 1873 K and stress range of 140–250 MPa.

3.2. Creep properties

Fig. 2 shows a typical time vs. elongation curve for single-crystal $\text{Al}_2\text{O}_3/\text{YAG}$ eutectic of 0° specimen to the solidified direction for a compressive creep test at 1873 K and stress range 140–250 MPa. In this figure elongation includes elastic and creep deformation. At a stress of 140 MPa, sufficient time is allowed to establish a secondary creep rate. After the secondary creep rate is reached, the stress is changed and primary and secondary creep rates are again measured at a stress of 200 MPa. The stress is increased up to 250 MPa. The eutectic composite used a specimen tested in compressive creep under a single condition; minimum creep rates were not distinguishable from multiple tests in the

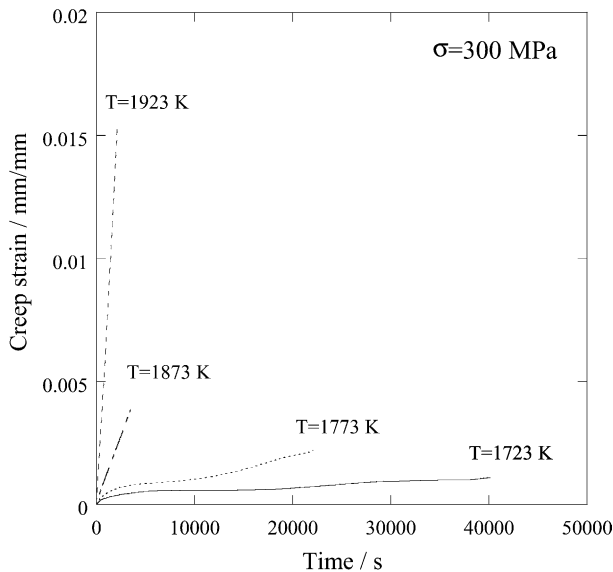


Fig. 3. Time vs. creep strain curves for single-crystal $\text{Al}_2\text{O}_3/\text{YAG}$ eutectic of 0° specimen to the solidified direction for a compressive creep test at 1723–1923 K and a stress of 300 MPa.

sense that the average value and the degree of scatter from the two test procedures were the same.

Fig. 3 shows time vs. creep strain curves of 0° specimen to the solidified direction for compressive creep tests at 1723–1923 K and a stress of 300 MPa. Each creep curve has a region of short primary creep and secondary creep, showing a normal creep curve similar to metallic systems. In the initial part of the curve, the creep rate decreases with increasing strain and reaches a minimum, achieving a brief quasi-steady state. Normally, the higher the temperature, the greater the creep rate. Here, the creep rate was defined as the minimum state (i.e., minimum creep rate).

Fig. 4 (a) shows the stress dependence of the minimum creep rate for single-crystal $\text{Al}_2\text{O}_3/\text{YAG}$ eutectic of 0° specimen to the solidified direction for compressive creep tests at 1723–1923 K. Minimum creep rates increase with increasing applied stresses, according to a power-law relationship. The creep rate, $\dot{\epsilon}$, is related to applied stress, σ , by the following relationship:

$$\dot{\epsilon} = A\sigma^n \exp\left(-\frac{Q}{RT}\right)$$

where A is a material constant, n is the stress exponent, Q is the activation energy for creep, R is the gas constant and T is the absolute temperature. The minimum creep rate was reached after a very short primary stage (e.g., about 0.08% at 1923 K and 140 MPa). The figure shows that the stress exponent of the 0° specimen decreases with increasing temperatures (from $n=10$ at 1723 K to $n=7.3$ at 1773 K, $n=5.8$ at 1873 K, and 5.4 at 1923 K). Apparent activation energies for creep deformation are obtained from the slope of semi-logarithmic Arrhenius plots of creep rate vs. inverse temperature as shown in Fig. 4(b). Activation energies for the 0° specimen are 810–986 kJ/mol over the stress range of 200–350 MPa.

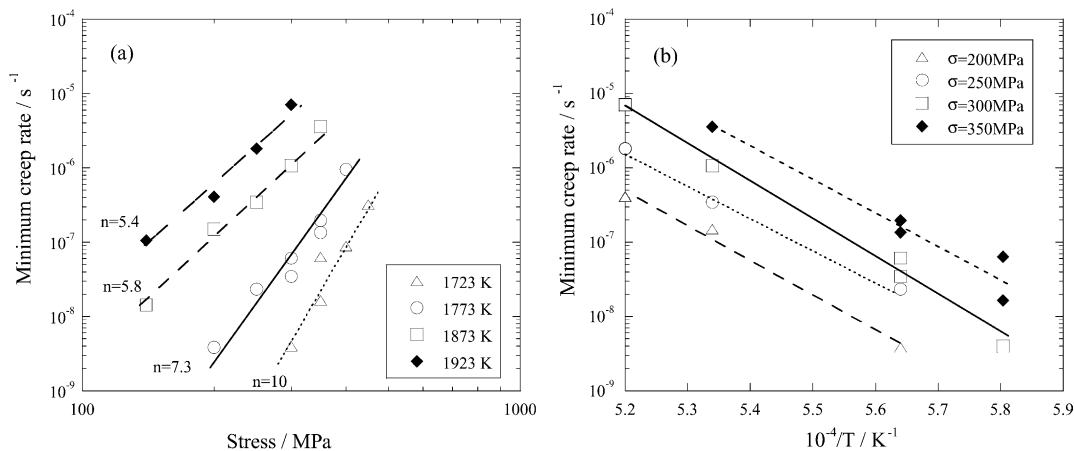


Fig. 4. (a) Minimum creep rate as a function of stress at temperatures of 1723–1923 K for single-crystal $\text{Al}_2\text{O}_3/\text{YAG}$ eutectic of 0° specimen to the solidified direction. (b) Minimum creep rate as a function of inverse temperature.

Fig. 5(a) shows the stress dependence of the minimum creep rate for single-crystal $\text{Al}_2\text{O}_3/\text{YAG}$ eutectic of 90° specimen to the solidified direction for compressive creep tests at 1773–1923 K. Also plotted for comparison in Fig. 5(a) is that for the 0° specimen. The 90° specimen exhibits a slight increase in creep rate by about twice that of the 0° specimen over test temperature ranges. The stress exponent of the 90° specimen is about 7.6 at 1773 K; it decreases to 6.0 at 1873 K and 5.6 at 1923 K, which is close to that of the 0° specimen. Fig. 5(b) shows the minimum creep rate as a function of inverse temperature of the 90° specimen. The slope of Arrhenius plots indicates activation energies of 906–1024 kJ/mol over the stress range of 160–300 MPa. Table 1 summarizes activation energies for single-crystal $\text{Al}_2\text{O}_3/\text{YAG}$ eutectic of 0° and 90° specimens.

3.3. Dislocation structure

Fig. 6 shows bright field TEM images of single-crystal $\text{Al}_2\text{O}_3/\text{YAG}$ eutectic of 0° specimen to the solidified direction after 2.6% deformed on compressive creep test at 1873 K and stress of 350 MPa. As shown in Fig. 6(a) and (b), the dislocation structure is observed in both Al_2O_3 and YAG phase, indicating that creep deformation occurred by dislocation motion. Characteristic glide and climb of dislocation are observed, indicating a rate-controlling mechanism for ultra-high temperature deformation in single-crystal $\text{Al}_2\text{O}_3/\text{YAG}$ eutectic. In single-crystal Al_2O_3 , $(0001)1/3 \langle 11\bar{2}0 \rangle$ basal slip is the

easiest slip system to activate at high temperature.^{8,9} As shown in Fig. 6(a), the $\langle 11\bar{2}0 \rangle$ -basal slip is observed in Al_2O_3 phase. Also, in single-crystal YAG, dominant dislocations exhibit $\langle 111 \rangle$ -slip systems.¹⁰ However, as Fig. 6(b) shows, most dislocations observed in YAG phase are $\langle 110 \rangle$ -type and $\langle 100 \rangle$ -type. Dislocation density differs remarkably between Al_2O_3 and YAG phases. The sample after creep shows high dislocation motion in Al_2O_3 and moderate motion in the YAG phase. Fig. 6(c) shows that dislocation of $\text{Al}_2\text{O}_3/\text{YAG}$ phase boundary becomes sessile. It is assumed that one possible source for back-stress source is an Orowan pile-up and bowing mechanism^{11,12} occurring in Al_2O_3 matrix due to the presence of higher creep resistance in YAG phase.

3.4. Creep behavior of single-crystal $\text{Al}_2\text{O}_3/\text{YAG}$ eutectic

As shown in Figs. 4(a) and 5(a), creep data of single-crystal $\text{Al}_2\text{O}_3/\text{YAG}$ eutectic follows a power-law relationship. Dislocation structure is observed in both Al_2O_3 and YAG phase (see Fig. 6), illustrating such creep behavior characterized by dislocation creep and coarse-grained oxides (with little or no grain boundary). Reportedly, basal slip systems in single-crystal Al_2O_3 are activated at temperatures of 1173 K; the prismatic system is activated above 1423 K.^{8,9} Creep deformation occurs by dislocation above 1773 K for single-crystal YAG.¹⁰ Stress exponents of single-crystal $\text{Al}_2\text{O}_3/\text{YAG}$

Table 1
Experimental activation energies for compressive creep of single-crystal $\text{Al}_2\text{O}_3/\text{YAG}$ eutectic

Specimen	Direction	Test temperature/K	Activation energy, Q/kJ/mol				
			160 MPa	200 MPa	250 MPa	300 MPa	350 MPa
Single-crystal $\text{Al}_2\text{O}_3/\text{YAG}$ eutectic	$[11\bar{2}0]/[210]$	1723–1923	–	903	810	986	842
	90° to $[11\bar{2}0]/[210]$	1773–1923	1018	1024	926	906	–

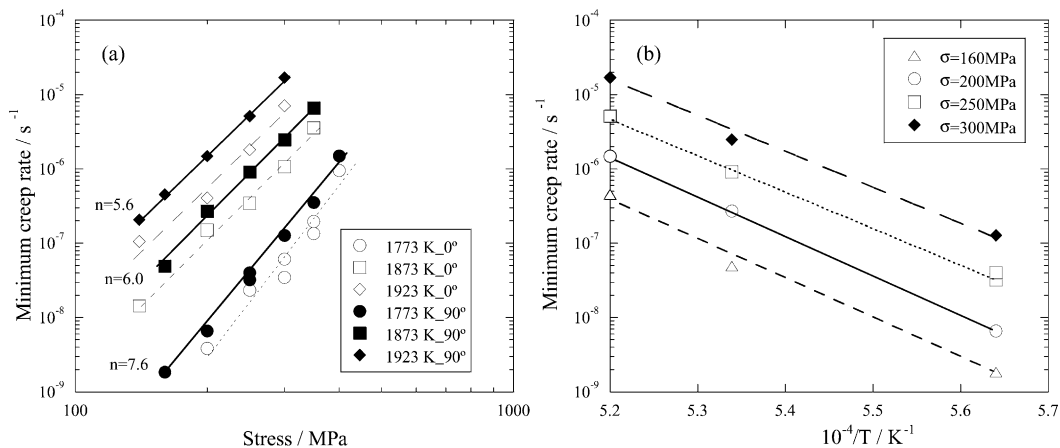


Fig. 5. (a) Minimum creep rate as a function of stress at temperatures of 1773–1923 K for single-crystal $\text{Al}_2\text{O}_3/\text{YAG}$ eutectic of 90° specimen to the solidified direction, together with that of 0° specimen. (b) Minimum creep rate as a function of inverse temperature.

eutectic are: 5.4–10 ($n=5.4$ –10 for 0° specimen and $n=5.6$ –7.6 for 90° specimen, to the solidified direction), close to values of $n=5$ –6 reported by Waku et al.^{1–3} on a constant strain rate compression test (CSRC); $n=5.0$ –5.5 for coarse-grained $\text{Al}_2\text{O}_3/\text{YAG}$ eutectic (nominal composition of alumina–18.5 mol% yttria fabricated by directional solidification, grain size: 2–3 mm) reported by Parthasarathy et al.¹³ on CSRC; $n=4.54$ –4.73 for single-crystal Al_2O_3 ;¹⁴ and $n=2.69$ –6.18 for single-crystal YAG on a constant load compression test (CLC) as reported by Corman^{14,15} (see Table 2).

As listed in Table 2, apparent activation energies for creep deformation are $Q=810$ –986 kJ/mol for 0° specimen and $Q=906$ –1024 kJ/mol for 90° specimen. These values are close to that for coarse-grained $\text{Al}_2\text{O}_3/\text{YAG}$ eutectic,¹³ 42° from c -axis single-crystal Al_2O_3 ¹⁴ and single-crystal YAG,^{14,15} and also that of self-diffusion for single-crystal Al_2O_3 ,^{16,17} but more than twice that for creep of c -axis single-crystal Al_2O_3 ¹⁴ and more than thrice that for oxygen diffusion of single-crystal YAG¹⁸ (depending on heat treatment). This result suggests that ultra-high temperature deformation in single-crystal $\text{Al}_2\text{O}_3/\text{YAG}$ eutectic may be controlled by a dislocation motion induced by lattice diffusion in single-crystal Al_2O_3 or YAG.

Respective comparisons of creep behavior between single-crystal $\text{Al}_2\text{O}_3/\text{YAG}$ eutectic and coarse-grained $\text{Al}_2\text{O}_3/\text{YAG}$ eutectic, single-crystal Al_2O_3 , and single-crystal YAG are shown in Fig. 7. The creep rate of single-crystal $\text{Al}_2\text{O}_3/\text{YAG}$ eutectic, at a given stress, is lowered by more than two orders of magnitude for coarse-grained $\text{Al}_2\text{O}_3/\text{YAG}$ eutectic at 1923 K,¹³ about six for 42° from c -axis single-crystal Al_2O_3 ,¹⁴ and about one order of magnitude for a -axis single-crystal Al_2O_3 fiber at 1873 K.⁹ An equivalent observation is that single-crystal $\text{Al}_2\text{O}_3/\text{YAG}$ eutectic has the same creep rate at 1923 K and a given stress as c -axis single-crystal Al_2O_3 .¹⁴ However, creep resistance of single-crystal YAG^{14,15} exceeds that of single-crystal $\text{Al}_2\text{O}_3/\text{YAG}$ eutectic at 1873 K. Because of the relationship in creep rate as a function of stress between a -axis single-crystal Al_2O_3 and $[110]$ single-crystal YAG, the single-crystal $\text{Al}_2\text{O}_3/\text{YAG}$ eutectic can be well simplified such that the composite consists of an unidirectional structure of each phase, related to describe a simple isostrain model for the composite.¹⁹

3.5. Larson–Miller procedure for creep data

The basis of the Larson–Miller method^{20,21} is that the creep process can be considered to be thermally activated. Consequently, the creep rate is described by an Arrhenius plot for a given applied stress;

$$\dot{\varepsilon} = B \exp\left(-\frac{Q}{RT}\right) \quad (2)$$

Table 2

Creep properties for $\text{Al}_2\text{O}_3/\text{YAG}$ eutectic composites, single-crystal Al_2O_3 and single-crystal YAG, together with data of self-diffusion for single-crystal Al_2O_3 and single-crystal YAG

Specimen	Direction	Test temperature/K	Applied stress/MPa	Method	Test atmosphere	Stress exponent	Activation energy/kJ/mol	References
Single-crystal $\text{Al}_2\text{O}_3/\text{YAG}$ eutectic (Al_2O_3 –18.0 mol% Y_2O_3)	$[11\bar{2}0]/[210]$	1723–1923	140–450	CLC	Air	5.4–10	810–986	This work
	90° to $[11\bar{2}0]/[210]$	1773–1923	140–400	CLC	Air	5.6–7.6	906–1024	This work
	$[11\bar{2}0]/[210]$	1773–1973	150–560	CSRC	Ar	5.0–6.0	670–905	Waku ^{1–3}
	$[11\bar{2}0]/[210]$	1773–1873	100–160	CLT	Air	8.0–10.0	600–1000	Harada ⁷
Coarse-grained $\text{Al}_2\text{O}_3/\text{YAG}$ eutectic (Al_2O_3 –18.5 mol% Y_2O_3)	Poly-crystal (2–3 mm)	1683–1923	200–436	CSRC	Air	5.0–5.5	650–800	Parthasarathy ¹³
	$[0001]$	1923–2123	140–400	CLC	He	4.54	470	Corman ¹⁴
	42° to $[0001]$	1473–1973	25–100	CLC	He	4.73	736	Corman ¹⁴
Single-crystal Al_2O_3	$[0001]$	1773–1993	–	O^{18} self-diffusion, SIMS	–	–	636–896	Prot ¹⁶
	$[0001]$	1813–1970	–	Al^{26} self-diffusion, SIMS	–	–	510–850	Le Gall ¹⁷
	$[100]$	1923–2123	100–280	CLC	He	2.69	674	Corman ^{14,15}
	$[110]$	1923–2123	50–280	CLC	He	6.18	650	Corman ^{14,15}
	$[111]$	1923–2123	100–280	CLC	He	5.64	710	Corman ^{14,15}
Single-crystal YAG	$[111]$	1313–1813	–	O^{18} self-diffusion, SIMS	–	–	297–325	Hanedat ¹⁸

CLC: Constant Load Compression; CSRC: Constant Strain Rate Compression; CLT: Constant Load Tension; SIMS: Secondary Ion Mass Spectrometry.

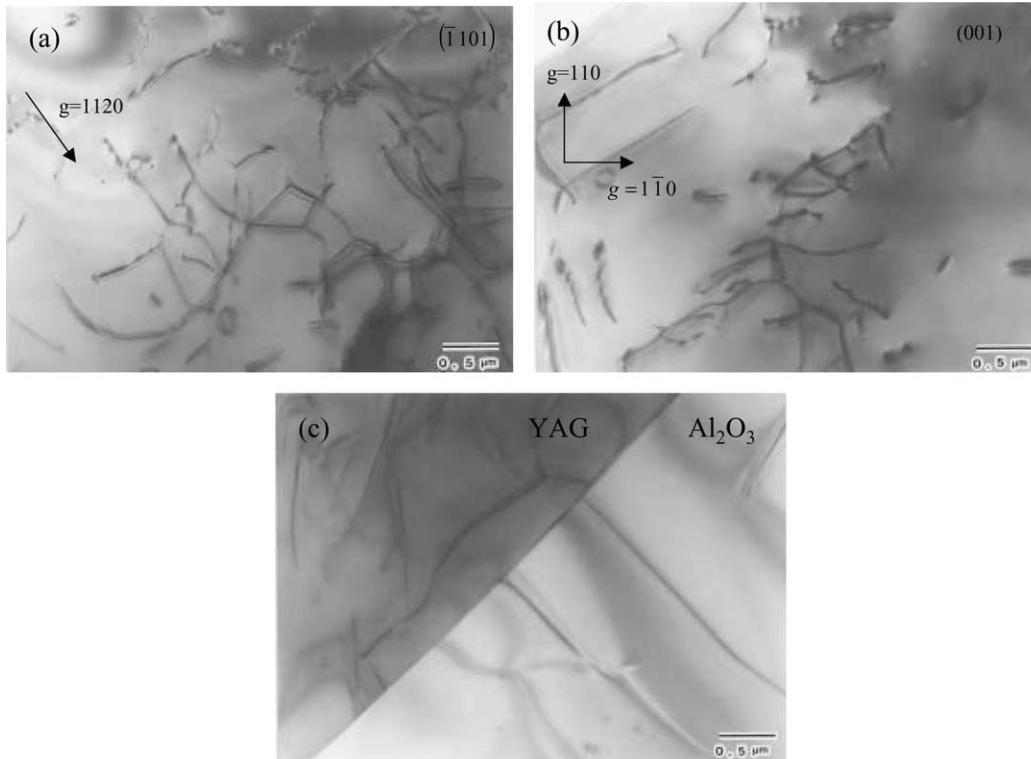


Fig. 6. TEM images showing dislocation structures of (a) Al_2O_3 phase, (b) YAG phase and (c) phase boundary in single-crystal $\text{Al}_2\text{O}_3/\text{YAG}$ eutectic of 0° specimen to the solidified direction after 2.6% deformed on compressive creep test at 1873 K and a stress of 350 MPa.

where B is a constant. Eq. (2) can also be written as

$$\frac{Q}{R} = T(\ln B - \ln \dot{\epsilon}). \quad (3)$$

Introducing the concept of creep life, t_s , defined as the time taken for the steady creep rate to yield a given arbitrary strain, ϵ_x , is

$$t_s = \frac{\epsilon_x}{\dot{\epsilon}}. \quad (4)$$

Eq. (3) can then be written as

$$L = \frac{Q}{R} = T(C + \log t_s), \quad (5)$$

where L is the Larson–Miller parameter and C is a constant. Creep data appropriate to other combinations of stress-temperature-lifetime can be predicted from the Larson–Miller plot by interpolation or extrapolation. For example, Larson–Miller plots were used in the present work to derive creep strength defined as the stress required at 1873 K to produce a strain, ϵ_x , of 10^{-3} in a time, t_s , of 10^6 s. (i.e., $\dot{\epsilon} = 10^{-9}$).

Fig. 8 shows the Larson–Miller parameter derived from stated C values using Eq. (5) plotted versus corresponding values of stress for single-crystal $\text{Al}_2\text{O}_3/\text{YAG}$ eutectic of 0° and 90° specimens to the solidified direction. Linear regression was used to postulate a straight line through the data. These data well fit $C=23$ linearly.

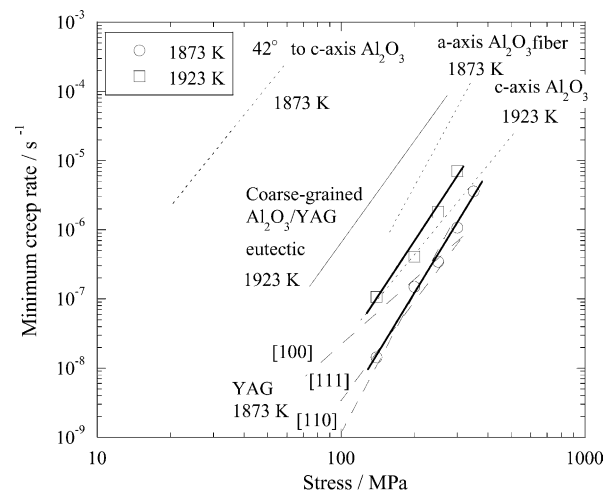


Fig. 7. Comparison of creep behavior between single-crystal $\text{Al}_2\text{O}_3/\text{YAG}$ eutectic and coarse-grained $\text{Al}_2\text{O}_3/\text{YAG}$ eutectic, single-crystal Al_2O_3 , and single-crystal YAG.

Constructed lines were used to obtain creep strength, i.e., stress corresponding to $t_s = 10^6$ s at a temperature of 1873 K. Values of t_s and T give a Larson–Miller parameter of $L = 54317$ which yields, by extrapolation, creep strengths of 96 and 82 MPa for 0° and 90° specimens, respectively. Creep resistance decreases slightly in the sample with 90° deviation from 0° -axis loading, but it exhibits moderate strength. Table 3 summarizes creep strength evaluated by the Larson–Miller procedure.

Table 3
Creep strength for Al₂O₃/YAG eutectic composites, single-crystal Al₂O₃ and single-crystal YAG determined by Larson-Miller procedure

Specimen	Direction	Test temperature/K	Applied stress/MPa	Test method	Test atmosphere	°C	Creep strength/MPa	References
Single-crystal Al ₂ O ₃ /YAG eutectic (Al ₂ O ₃ –18.0 mol%Y ₂ O ₃)	[11 $\bar{2}$ 0]/[210]	1723–1923	140–450	CLC	Air	23	96	This work
	90° to [11 $\bar{2}$ 0]/[210]	1723–1923	140–400	CLC	Air	23	82	This work
Coarse-grained Al ₂ O ₃ /YAG eutectic (Al ₂ O ₃ –18.5 mol%Y ₂ O ₃)	Poly-crystal (2–3 mm)	1683–1923	200–436	CSRC	Air	21	2.0	Parthasarathy ¹³
Single-crystal Al ₂ O ₃	[0001]	1923–2123	140–400	CLC	He	11	73	Corman ¹⁴
	42° to [0001]	1473–1973	25–100	CLC	He	22	3.8	Corman ¹⁴
Single-crystal YAG	[100]	1923–2123	100–280	CLC	He	20	81	Corman ^{14,15}
	[110]	1923–2123	50–280	CLC	He	20	116	Corman ^{14,15}
	[111]	1923–2123	100–280	CLC	He	20	140	Corman ^{14,15}

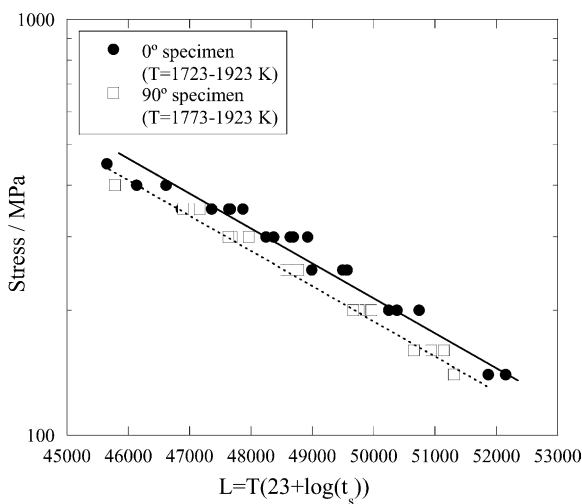


Fig. 8. Larson–Miller plot for single-crystal Al₂O₃/YAG eutectic of 0° and 90° specimens to the solidified direction.

Single-crystal Al₂O₃ has creep strengths of 73 and 3.8 MPa for [0001] and 42° from [0001] specimens, indicative of extreme anisotropy. Single-crystal YAG exhibits high strength with less anisotropy. The extreme anisotropy of single-crystal Al₂O₃ presumably originates in anisotropy of crystal structure and atomic bonding. Slight anisotropy of single-crystal Al₂O₃/YAG eutectic corresponds with results from that in single-crystal Al₂O₃. The coarse-grained Al₂O₃/YAG eutectic has quite low strength of 2.0 MPa because of the presence of grain boundaries or colonies between Al₂O₃ and YAG.

4. Conclusion

Compressive creep behaviors of in-situ single-crystal oxide Al₂O₃/YAG eutectic composite of 0 and 90° specimen to the solidified direction were studied in the temperature range 1723–1923 K and stress range 140–450 MPa. The following conclusions were reached:

1. The single-crystal Al₂O₃/YAG eutectic exhibits a stress exponent of 5.4–10 and a short primary creep behavior, indicative of compressive creep characterized by the dislocation mechanism. Activation energies for creep are 810–1024 kJ/mol, close to that for 42° from *c*-axis single-crystal Al₂O₃ or single-crystal YAG, in agreement with that of self-diffusion for *c*-axis single-crystal Al₂O₃.
2. The 0° specimen exhibits a slightly decreased creep rate by about half for the 90° specimen. This corresponds to results from crystal anisotropy in single-crystal Al₂O₃.
3. Dislocation structure is seen both in Al₂O₃ and YAG phase, indicating that creep deformation arose from dislocation motion. Dislocation density differs remarkably from that showing high dislocation motion in Al₂O₃ and moderate motion in YAG phase.
4. The single-crystal Al₂O₃/YAG eutectic displays superior creep resistance for coarse-grained Al₂O₃/YAG eutectic and 42° from *c*-axis single-crystal Al₂O₃. Still, creep resistance for single-crystal YAG slightly exceeds that of single-crystal Al₂O₃/YAG eutectic.
5. The Larson–Miller method provides an effective means of comparing creep resistance of oxides on the basis of results obtained under different stresses and temperatures.

Acknowledgements

This research was supported by Industrial Technology Research Grant Program in 2001 from New Energy and Industrial Technology Development Organization (NEDO) of Japan. We also acknowledge Dr. S. Sakata (Ube Co. Ltd.) for preparing test samples and Sumitomo Metal Technology Inc. for TEM observation.

References

1. Waku, Y., Nakagawa, N., Ohtsubo, H., Ohsora, Y. and Kohtoku, Y., High temperature properties of unidirectionally solidified Al_2O_3 -YAG composites. *J. Japan Inst. Metals*, 1995, **59**, 71–78.
2. Waku, Y. and Sakuma, T., Dislocation mechanism of deformation and strength of Al_2O_3 -YAG single crystal composites at high temperatures above 1500 °C. *J. Eur. Ceram. Soc.*, 2000, **20**, 1453–1458.
3. Waku, Y., Nakagawa, N., Wakamoto, T., Ohtsubo, H., Shimizu, K. and Kohtoku, Y., The creep and thermal stability characteristics of a unidirectionally solidified Al_2O_3 /YAG eutectic composite. *J. Mater. Sci.*, 1998, **33**, 4943–4951.
4. Waku, Y., High temperature characteristics of melt growth composites with a novel microstructure. *J. Japan Inst. Metals*, 2000, **64**, 977–984.
5. Waku, Y., High temperature properties and thermal stability of a unidirectionally solidified $\text{Al}_2\text{O}_3/\text{Er}_3\text{Al}_5\text{O}_{12}$ eutectic composite. *J. Japan Inst. Metals*, 2000, **64**, 101–107.
6. Waku, Y., Sakata, S., Mitani, A. and Shimizu, K., High-temperature strength and a microstructure of an $\text{Al}_2\text{O}_3/\text{Er}_3\text{Al}_5\text{O}_{12}/\text{ZrO}_2$ ternary MGC. *J. Japan Inst. Metals*, 2000, **64**, 1263–1268.
7. Harada, Y., Suzuki, T., Hirano, K. and Waku, Y., Influence of moisture on ultra-high temperature tensile creep behavior of in-situ single-crystal oxide ceramic Al_2O_3 /YAG eutectic composite. *J. Am. Ceram. Soc.*, 2003, **86**, 951–958.
8. Firestone, R. F. and Heuer, A. H., Creep deformation of 0° sapphire. *J. Am. Ceram. Soc.*, 1976, **59**, 24–29.
9. Kotchick, D. M. and Tressler, R. E., Deformation behavior of sapphire via the prismatic slip system. *J. Am. Ceram. Soc.*, 1980, **63**, 429–434.
10. Blumenthal, W. R. and Phillips, D. S., High-temperature deformation of single-crystal yttrium–aluminum garnet (YAG). *J. Am. Ceram. Soc.*, 1996, **79**, 1047–1052.
11. Strudel, J. L., Mechanical properties of multiphase alloys. In *Physical Metallurgy*, ed. R. W. Cahn and P. Haasen. Elsevier Science, Amsterdam, 1983, pp. 1481.
12. Legzdina, D. and Parthasarathy, T. A., Deformation mechanisms of a rapidly solidified Al–8.8Fe–3.7Ce alloy. *Metall. Trans. A*, 1987, **18A**, 1713–1719.
13. Parthasarathy, T. A., Mah, T. and Matson, L. E., Deformation behavior of an Al_2O_3 - $\text{Y}_3\text{Al}_5\text{O}_{12}$ eutectic composite in comparison with sapphire and YAG. *J. Am. Ceram. Soc.*, 1993, **76**, 29–32.
14. Corman, G. S., High-temperature creep of some single crystal oxides. *Ceram. Eng. Sci. Proc.*, 1991, **12**, 1745–1766.
15. Corman, G. S., Creep of yttrium aluminum garnet single crystals. *J. Mater. Sci. Lett.*, 1993, **12**, 379–382.
16. Prot, D. and Monty, C., Self-diffusion in alpha- Al_2O_3 . 2. Oxygen diffusion in ‘undoped’ single crystals. *Phillos. Mag. A*, 1996, **73**, 899–917.
17. Le Gall, M., Lesage, B. and Bernardini, J., Self-diffusion in alpha- Al_2O_3 . 1. Aluminum diffusion in single-crystals. *Phillos. Mag. A*, 1994, **70**, 761–773.
18. Haneda, H., Miyazawa, Y. and Shirasaki, S., Oxygen diffusion in single-crystal yttrium aluminum garnet. *J. Cryst. Growth*, 1984, **68**, 581–588.
19. Yoshida, H., Nakamura, A., Sakuma, T., Nakagawa, N. and Waku, Y., Anisotropy in high-temperature deformation in unidirectionally solidified eutectic Al_2O_3 -YAG single crystal. *Scripta Mater.*, 2001, **45**, 957–963.
20. Larson, F. R. and Miller, J., A time–temperature relationship for rupture and creep stresses. *Trans. ASME*, 1952, **74**, 765–771.
21. Deng, S. and Warren, R., Creep properties of single crystal oxides evaluated by a Larson–Miller procedure. A time-temperature relationship for rupture and creep stresses. *J. Eur. Ceram. Soc.*, 1995, **20**, 1453–1458.